

# Common Mode EMC Input Filter Design for a Three-Phase Buck-Type PWM Rectifier System

T. Nussbaumer, M. L. Heldwein and J. W. Kolar

Swiss Federal Institute of Technology (ETH) Zurich  
 Power Electronic Systems Laboratory  
 ETH Zentrum / ETL H23, Physikstrasse 3  
 CH-8092 Zurich / SWITZERLAND / Europe  
 heldwein@lem.ee.ethz.ch

**Abstract** — The EMC input filter design for a three-phase PWM rectifier is usually separated into the design of the differential (DM) and of the common mode (CM) stage. While for the DM filter part design rules and procedures are well-known and the parameters are easier to derive, the CM filter design is often based on trial-and-error methods and/or on the experience of the designer. In this work, a comprehensive design procedure for a CM EMC input filter is performed exemplarily for a three-phase three-switch buck-type PWM rectifier with an integrated boost output stage. A simplified model of the CM noise propagation is developed and the relevant parasitic impedances are identified. A capacitive connection from the star-point of the DM input filter to the capacitive centre point of the rectifier output voltage is proposed and the effect of this measure concerning CM EMC is verified. Finally, a two stage CM filter is designed and the compliance to the conducted emission requirements of CISPR 22 Class A is verified through measurements on a 5 kW prototype.

## I. INTRODUCTION

Three-phase buck-type PWM rectifier systems (also known as current source rectifiers, cf. **Fig.1**, [1]) are frequently employed as front-end converters in utility interfaced systems such as power supplies for telecommunication systems, process technology and AC drive applications. For the case at hand the power converter is intended to supply IT equipment and for such an application the limits stated in CISPR22 for Class B equipments [2] apply and are the aim of the present work.

Due to the discontinuous input currents of the system [1] at least a single-stage LC differential mode (DM) input filter is obligatory, however, for full compliance to EMC standards [3] the conducted DM and common mode (CM) conducted emissions (CE) propagating to the mains have to be attenuated sufficiently. Since the DM filter mainly defines the power density, the low-load power factor and the dynamics of the system, it is advantageous to design this filter stage in a first step, by employing either a numerical calculation procedure or using a CM/DM separator as presented in [4] for the buck-rectifier

system. For the rectifier used here, the DM filter stage designed in [4] is used.

The second step, the CM filter design is, in practice, often based on a trial-and-error and/or on the experience of the designer due to the inherently difficult prediction of the CM noise source characteristics in complex power electronics systems [3][5]. Accurate models for prediction have been proposed for boost-type rectifiers [6][7][8], where a relatively high effort is put on the numerical or mathematical modeling of the noise paths and sources. However, if a first prototype of the system is available, which can be used for the EMC evaluation, a simplified model of the CM noise propagation paths can also be achieved through the direct measurement of parasitic impedances of the system components [10]. Thus, the emission levels can be predicted with the necessary accuracy and the attenuation requirements for a CM input filter can be identified. For the case at hand the boost stage is not operating, but the capacitive connection between the semiconductors  $S_B$  and  $D_B$  are taken into consideration.

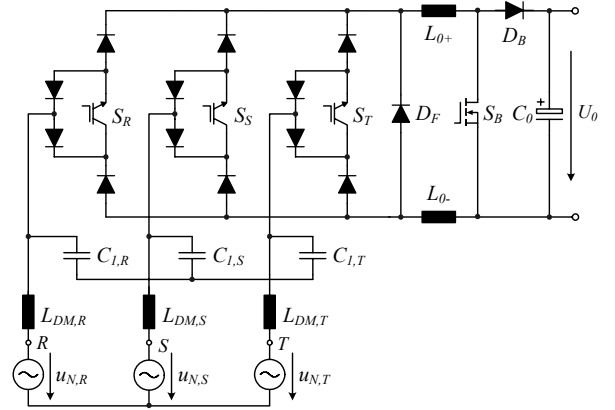


**Fig.1:** Structure of the power circuit of a three-phase three-switch buck PWM rectifier with integrated boost output stage designed as the input stage of a 5 kW telecommunications power supply switching at 28 kHz. For clarity, only the DM filter components [4] that are relevant for the CM filter design ( $L_{DM,i}$  and  $C_{l,i}$ ) are shown, where  $L_{DM,i}$  is the sum of all DM filter phase inductances.

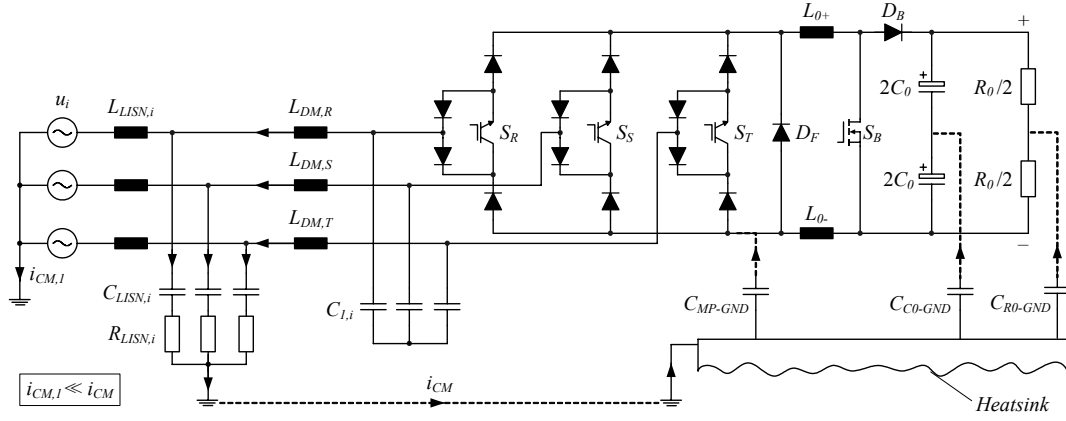


**Fig.2:** Propagation model of the common mode currents in the rectifier system used for deriving the CM noise model.

This work presents the different tasks performed for the CM filter design and evaluation, starting in **Section II**, where a simplified equivalent CM noise propagation model is developed and the relevant parasitic capacitances are identified through impedance measurements. The effect of a HF connection of the star-point of the DM input filter capacitors to the output of the rectifier is analyzed in **Section III** concerning its effect on the modeled CM noise paths. A two-stage conventional CM input filter is designed in **Section IV**, which presents the selection of the filter components aiming to achieve the filter's required attenuation. Furthermore, the damping effect and/or insertion loss of the employed filter elements is analyzed. Finally, in **Section V** the compliance to CISPR 22 Class B limits is verified through CE measurements on a 5 kW prototype employing the proposed CM filter.

## II. COMMON MODE NOISE PROPAGATION MODELING

A simplified circuit model for the CM noise propagation paths and sources is developed (cf. **Fig.3**), which sets the basis for the identification of the filtering requirements and the analysis of the effect of the placement of the filtering elements. The main propagation paths of the CM current are shown in

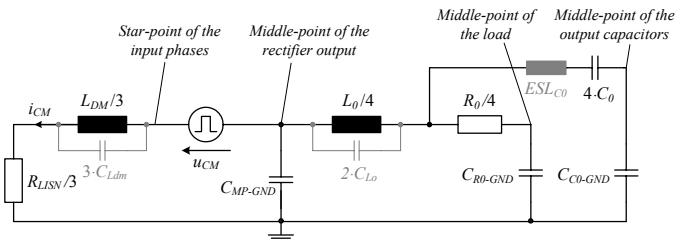


**Fig.3:** CM noise propagation model for the three-phase buck-type PWM rectifier with integrated boost output stage. Components values:  $L_{DM} = 270 \mu\text{H}$ ;  $L_0 = 2 \text{ mH}$ ;  $C_0 = 750 \mu\text{F}$ ;  $C_{MP-GND} = 141 \text{ pF}$ ;  $C_{R0-GND} = 57 \text{ pF}$ ;  $C_{C0-GND} = 283 \text{ pF}$ .

**Fig.2** through lumped capacitances from the components to the heatsink, which for the system at hand is connected to the power distribution protective earth (PE). The common mode current  $i_{CM}$  flowing through the three phases and the three DM filter inductors to the mains causes an according noise level at the supplying mains and/or LISN network (in case of the CE testing process). Assuming, due to  $L_{LISN,i}$  at high frequencies, an ideal decoupling of the EUT to the mains, and a perfect coupling with the test receiver, through  $C_{LISN,i}$  in a simplified consideration, the equivalent high frequency circuit **Fig.3** is obtained and used in the following analysis.

The CM current path is closed through the parasitic capacitances ( $C_{MP-GND}$ ,  $C_{C0-GND}$  and  $C_{R0-GND}$ ) between the PE terminal, the heatsink and the elements of the power circuit. For the CM current the three phases are lying in parallel, therefore, one third of the DM input filter inductor value becomes effective as depicted in **Fig.3**, and one third of the test receiver sensing input resistance  $R_{LISN,i}$  is seen by the common mode current. The capacitance  $C_{MP-GND}$  is the lumped capacitance model for the high frequency connection between the power modules ( $S_R$ ,  $S_S$ ,  $S_T$ ) and the heatsink. It is drawn in **Fig.2** in the negative rail since a higher capacitance is observed at the anodes of the diodes.

Still regarding CM paths, on the DC side of the rectifier circuit, the two DC inductances  $L_{0+} = L_0 = L_0/2$  are lying in parallel. If the capacitances from the output capacitors to ground, which are distributed parasitic capacitances, are summed into a single total capacitance  $C_{C0-GND}$ , one path with output capacitance  $C_0$  results and this path is modeled with the equivalent series inductance  $ESL_{CO}$  of the output electrolytic capacitors. The capacitance  $C_{C0-GND}$  models the influence of the parasitic capacitive connection from the boost switch  $S_B$  and diode  $D_B$  to the heatsink, once the output capacitors are seen as low impedances for high frequency current components. The distributed capacitances from the load resistor to ground are

modeled through  $C_{R0-GND}$  from the load middle-point to ground which results in a path with  $R_0/4$ .

The rectifier itself is modeled as a common mode voltage source  $u_{CM}$  that drives the potential between the star-point of the rectifier input (lying at the star-point of the DM input filter capacitors, which are not relevant for the CM noise model) and the middle-point of the rectifier output.

Furthermore, the parasitic capacitances from the differential mode filter inductors  $C_{Ldm}$  and from the output inductors  $C_{Lo}$  are not taken into consideration because their resonance frequency is above 1 MHz. In a more detailed model, where emissions at higher frequencies are to be attenuated, these parameters are of great importance and should not be discounted.

For the measurement and estimation of the relevant capacitances ( $C_{MP-GND}$ ,  $C_{CO-GND}$  and  $C_{R0-GND}$ ), three impedance measurements are performed with an impedance analyzer Agilent 4294A, well suited for the relevant frequency range. For evaluating  $C_{R0-GND}$  a simple impedance measurement is carried out with disconnected power cables leading to a high frequency equivalent circuit presenting a resistor, an inductor and a capacitor in series, from which only the capacitance value is used in this design procedure and has a value of  $C_{R0-GND} = 57$  pF.

The mathematical estimation of the relevant capacitances  $C_{MP-GND}$  and  $C_{CO-GND}$  is performed through two impedance measurements. The rectifier is disconnected from the mains and the load and the impedances  $Z_{MP-GND}$  and  $Z_{CO-GND}$  are measured according to the setup shown in Fig.4. The results from these measurements are presented in Fig.5. Simple equivalent C-L-R circuits are taken as approximation within the frequency range close to 600 kHz due to the high order

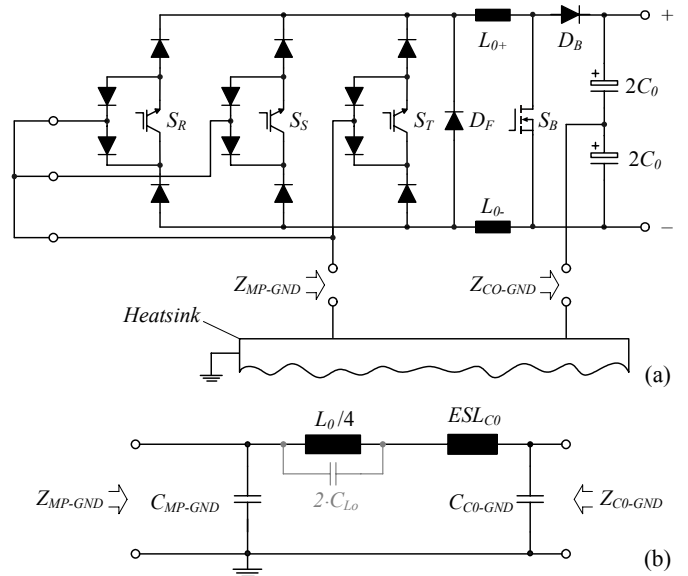


**Fig.4:** Setup for the impedance measurements performed in order to evaluate the CM noise paths within the rectifier prototype. (a) Measurement setup. (b) Considered equivalent circuit for the calculation of the parasitic capacitances.

observed in the impedance measurements. As it is seen in Fig.6(b), the critical frequency range for the design of the CM filter is close to 600 kHz and it is for this frequency that the input CM filter is here designed.

By considering the two equivalent circuits (cf. Fig.4(b)) resulting from each impedance measurement, two equations for the two unknown parameters  $C_{MP-GND}$  and  $C_{CO-GND}$  can be derived, resulting in  $C_{CO-GND} = 283$  pF and  $C_{MP-GND} = 141$  pF. The resistive and inductive elements (L and R) also resulting from the calculations are neglected, and leads to a non-damped circuit model, which is used towards a worst case approximation for the filter design.

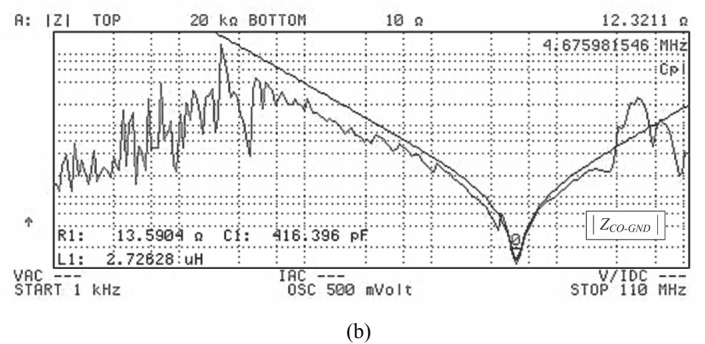
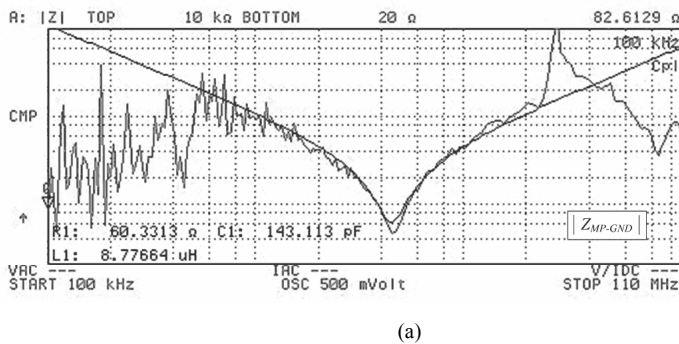


**Fig.5:** Impedance curve of the parasitic impedances (a)  $Z_{MP-GND}$  between the three shorted input phases and the ground potential and; (b)  $Z_{CO-GND}$  measured between the mid-point of the output capacitors and the ground potential.

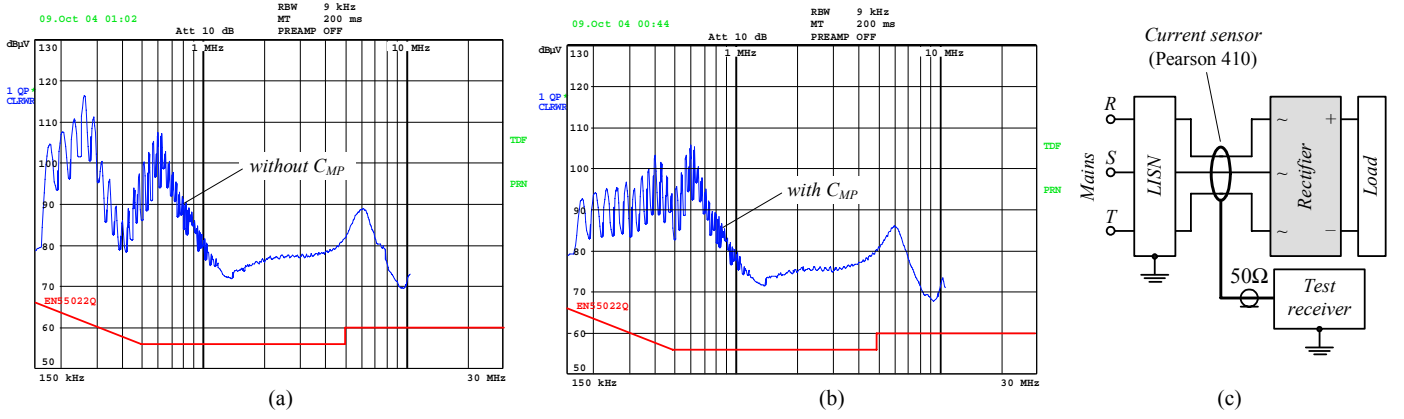


**Fig.6:** Effect of the capacitive connection ( $C_{MP}$ ) from the star-point of the DM input filter capacitors to the rectifier output with  $C_{MP} = 20$  nF. The sum of the input currents is measured with a Pearson 410 current probe in order to obtain only the CM signal. As the current measurement bandwidth is 20 MHz, the measurement is constrained to 10 MHz. **(a)** Conducted emissions measurement without the inclusion of CM filtering elements. **(b)** Measurement after the inclusion of the capacitive connection between the input star-point and the output DC-link through  $C_{MP}$ . **(c)** Simplified schematic for the measurement setup.

### III. EFFECTS OF A CAPACITIVE CONNECTION FROM THE INPUT STAR-POINT TO THE OUTPUT CENTER-POINT

The main purpose of the CM input filter is to hinder the common mode current propagation to the mains by providing a high impedance in the direction to the mains and/or by providing paths with low impedance around the rectifier elements, which are responsible for the generation of CM voltages so that CM noise current is circulated back internally. With that objective, an equivalent capacitor  $C_{MP}$  (cf. **Fig.7**) is placed between the star-point of the DM input filter capacitors and the center point of the output capacitors, allowing the HF common mode current to return in some extent to its source. In the case at hand,  $C_{MP} = 20$  nF was selected in order to shift the resonance at 250 kHz (cf. **Fig.6(a)**) to a lower frequency, lying below 150 kHz. In practice two capacitors  $C_{MP}/2 = 10$  nF have been connected to the positive and negative output capacitor terminals, respectively.

The effect of this connection is shown in **Fig.6** by CM CE measurements employing a Pearson 410 current probe, presenting a nominal bandwidth of 20 MHz, measuring the sum of the three input currents. The original CM CE measurement is shown in **Fig.6(a)**, where high emission levels are measured at 250 kHz and 600 kHz. In **Fig.6(b)** the measurement performed

with the inclusion of  $C_{MP}$  is presented and, as it can be noticed, the noise emission in the lower frequency range has been reduced, and especially the peak at 250 kHz has been shifted down to a lower frequency, sitting outside of the measurement range of interest.

Regarding the CE CM measurements, the current sensor produces an output signal of 0.05 V/A at an external 50  $\Omega$ -termination (which lies in parallel to the internal 50 $\Omega$ -termination of the sensor), which corresponds to an attenuation  $G_{Pearson}$  of

$$G_{Pearson} = 20 \cdot \log(0.05) = -26 \text{ dB} . \quad (1)$$

The measurement at the LISN resistance  $R_{LISN} / 3 = 50 \text{ } \Omega / 3$  appears with a gain  $G_{LISN}$  of

$$G_{LISN} = 20 \cdot \log(50/3) = 24.4 \text{ dB} . \quad (2)$$

Therefore, the gain of the measurement result with the current sensor  $G_{total}$  is given by

$$G_{total} = G_{LISN} - G_{Pearson} = 50.4 \text{ dB} , \quad (3)$$

accordingly the measurement curves are located 50.4 dB below the measurement level detected by the EMC test receiver. This gain also must be considered for the subsequent filter design.

### IV. TWO-STAGE COMMON MODE FILTER DESIGN

For guaranteeing compliance to EMC standards **Fig.6(b)** shows that, regarding common mode emissions, an attenuation of -50.4 dB around 600 kHz has to be provided by the CM filter (since **Fig.6** shows measurements employing the current sensor). Considering an additional margin of 6 dB for tolerances of the filter components an attenuation of

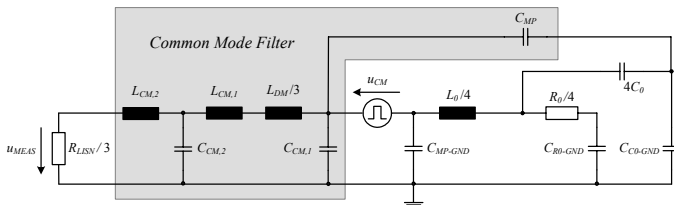


**Fig.7:** Two-stage CM filter (including the capacitive connection  $C_{MP}$  of input and output) for achieving the required attenuation of the CM emissions.

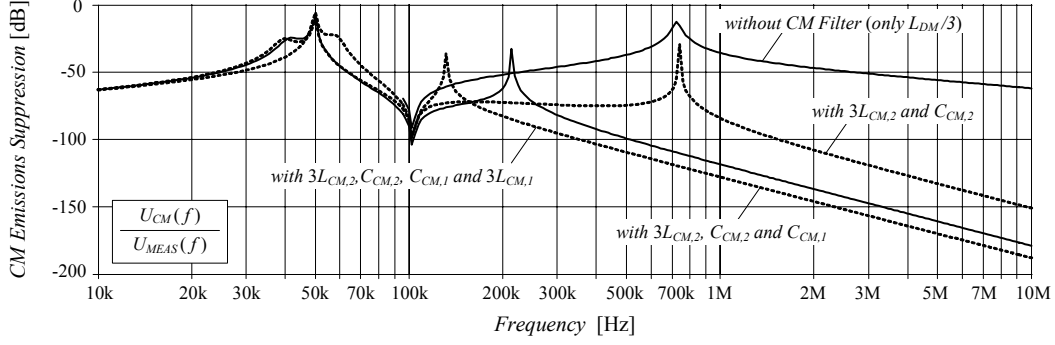


**Fig.8:** Attenuation plots for the circuit of Fig.7. Shown are the different attenuation curves of the transfer function  $U_{MEAS}(j\omega)/U_{CM}(j\omega)$  for different filter configurations, clarifying the effects of the insertion of each filtering element to the CM attenuation. The capacitance  $C_{MP}$  is included in all presented curves.

$$Att_{CM,req} = -56 \text{ dB} \quad (4) \quad \text{resulting in the inductors specified in Table I.}$$

at 600 kHz is selected. For reducing the total size of the CM filter the attenuation is distributed to two filter stages (in analogy to DM filter design procedures, see [4]) as presented in the following.

The total capacitance  $C_{CM,total} = C_{CM,1} + C_{CM,2}$  between any of the input phases and the PE is restrained by the maximum allowable earth leakage  $I_{GND,rms}$  current due to IT safety regulations. The tests are performed usually with 110 % of the input RMS voltage  $U_{N,rms}$  and the leakage current [12] should be typically limited to

$$I_{GND,rms} \leq 3.5 \text{ mA}, \quad (5)$$

even for the case where one of the phases is lost.

With the leakage current [12] given by

$$I_{GND,rms} = 1.1 \cdot U_{N,rms} \cdot 2\pi \cdot 50 \text{ Hz} \cdot C_{CM,total}, \quad (6)$$

a maximum of approximately  $C_{CM,total} \leq 44 \text{ nF}$  is reached. Providing a large margin and guaranteeing small footprints for the capacitors, the values of  $C_{CM,1} = C_{CM,2} = 4.7 \text{ nF}$  are selected. With two of the filter elements selected, the next step is the determination of the inductors. For that the total required attenuation  $Att_{CM,req}$  at 600 kHz is divided into two parts ( $Att_{CM,1}$  and  $Att_{CM,2}$ ),

$$Att_{CM,1} \cong -21 \text{ dB}, \quad (7)$$

$$Att_{CM,2} \cong -35 \text{ dB}. \quad (8)$$

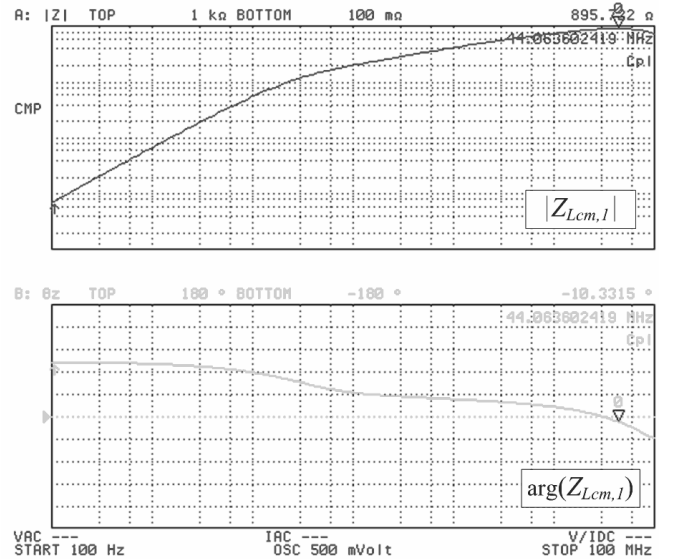
With these values the required impedances for the inductors  $L_{CM,1}$  and  $L_{CM,2}$  are calculated as

$$Z_{LCM,1,req} \cong 580 \Omega @ 600 \text{ kHz}, \quad (9)$$

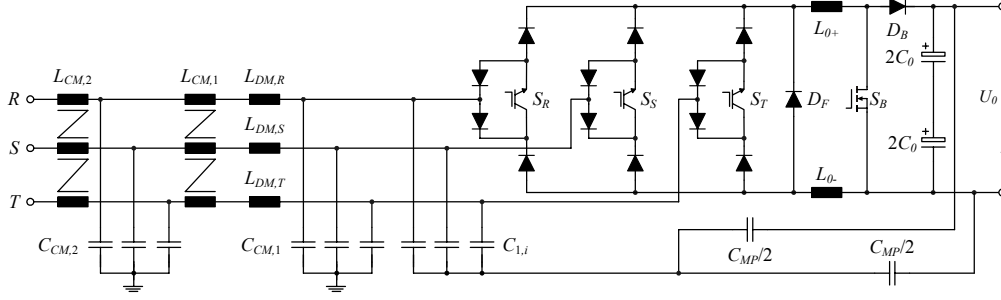
$$Z_{LCM,2,req} \cong 3 \text{ k}\Omega @ 600 \text{ kHz}, \quad (10)$$

TABLE I – SELECTED COMPONENTS FOR THE CM FILTER.

Component	Specification
$C_{CM,1}, C_{CM,2}$	Y1 Capacitor, Epcos MKP B81123 4.7nF – 250Vac
$C_{MP}$	Y1 Capacitor, Epcos MKP B81123 2 x 10nF – 250Vac
$L_{CM,1}$	Vacuumschmelze VAC VITROPERM 500F W409 N = 3 x 4 turns, AWG16
$L_{CM,2}$	Vacuumschmelze VAC VITROPERM 500F W380 N = 3 x 7 turns, AWG16



**Fig.9:** Impedance measurement for the inductor  $L_{CM,1}$ . A well damped high frequency behaviour and a high self resonance frequency ( $\cong 44 \text{ MHz}$ ) can be observed. The impedance at 600 kHz is measured as 490  $\Omega$ .



**Fig.10:** Final circuit structure for the three-phase PWM rectifier system including the designed CM input filter.

The effect of the addition of the filtering elements to the single-phase equivalent circuit of Fig.7 can be observed in **Fig.8** through the plots of the transfer function  $U_{MEAS}(j\omega)/U_{CM}(j\omega)$  for the different circuit configurations. It is observed that the final filter configuration is able to provide more than 60 dB attenuation at 600 kHz when compared to the original circuit.

Table I presents the specifications for all other components employed in the CM filter. Passive damping through resistors is not added due to the predominantly resistive high frequency behavior of the inductors (cf. **Fig.9**) that results from the losses in the core material (VITROPERM 500F). These inductors exhibit good impedance stability for high temperatures, high power density and high resonance frequency as well, and are therefore well suited for the CM filtering task.

## V. EXPERIMENTAL VERIFICATION

The final circuit schematic for the rectifier system including the CM filtering elements is shown in **Fig.10**. **Fig.11** shows the

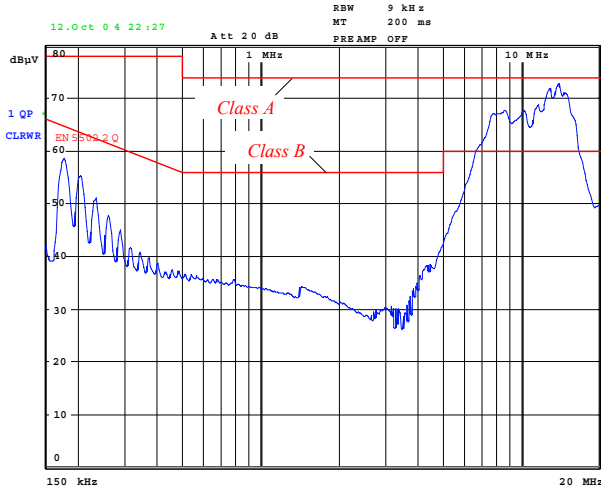


**Fig.11:** Conducted emissions measurement according to CISPR 22 of the rectifier ( $U_{N1-L,rms} = 400V$ ,  $U_0 = 400V$ ,  $P_0 = 5kW$ ) including the proposed CM filter and the DM filter. These measurements were performed at the output terminals from a LISN (not with a current transformer).

final result of the EMC CE measurement process performed with a four-line  $50\Omega/50\mu H$  LISN according to CISPR 16 [12]. The measurement is performed in order to test the full compliance of the rectifier and includes both common and differential mode emissions from the 5 kW hardware prototype of the system (cf. **Fig.12**). The noise emissions are mainly dominated by the DM noise emissions showing peaks at multiples of the switching frequency. Obviously, the CM noise emissions are attenuated sufficiently, and Class A is fulfilled in the frequency range 150 kHz – 20 MHz. For fulfilling Class B the emission levels that increase around 10 MHz would have to be properly attenuated what can be achieved through a shielding of the EMC input filter, as this is not implemented in the prototype.

## VI. CONCLUSIONS

In this work, a common mode filter for a three-phase PWM rectifier is designed based on a CM noise propagation model, which is parameterized by simple impedance measurements on an existing converter prototype. The model, along with a pre-

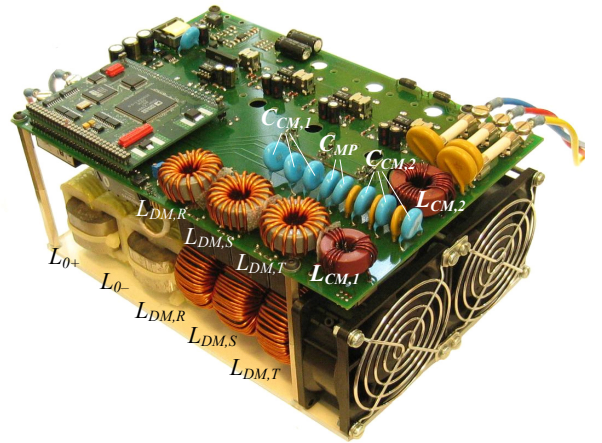


**Fig.12:** 5kW hardware prototype including the proposed CM filter, the DM filter, auxiliary power supply, and the DSP control board (160 mm x 240 mm x 120 mm).

vious CE EMC measurement, allows a sufficiently accurate prediction of the required CM filter attenuation and a straightforward design, with no complex modeling of the noise paths required. A capacitive connection between the star-point of the DM input filter capacitors and the output capacitor is proposed and additionally contributes to the attenuation of the common mode noise through the modification of the noise propagation path. The selection of the filtering elements is presented and their main characteristics are explained. Finally, measurements on a hardware prototype verify the theoretical considerations and the successful common mode filter design. With this work the HF modeling of the noise paths is performed in a simplified way, aiming for the reduction of the CM emissions at 600 kHz, but a further step extension of the modeling shall be implemented in future work with the objective of understanding all the relevant impedances.

#### REFERENCES

- [1] L. Malesani, and P. Tenti, "Three-Phase AC/DC PWM Converter with Sinusoidal AC Currents and Minimum Filter Requirements," *IEEE Transactions on Industry Applications*, vol. 23, no. 1, pp. 71-77, 1987.
- [2] IEC International Special Committee on Radio Interference – C.I.S.P.R., "Limits and Methods of Measurement of Radio Disturbance Characteristics of information Technology Equipment", Publication 22. Genève, Switzerland, 1993.
- [3] M.J. Nave, *Power Line Filter Design for Switched-Mode Power Supplies*, New York, USA: Van Nostrand Reinhold; 1991.
- [4] T. Nussbaumer, M.L. Heldwein, and J.W. Kolar, "Differential Mode EMC Input Filter Design for a Three-Phase Buck-Type Unity Power Factor PWM Rectifier," *Proceedings of the 4<sup>th</sup> International Power Electronics and Motion Control Conference*, Xian, China, pp. 1521-1526, 2004.
- [5] L. Yang, B. Lu, W. Dong, Z. Lu, M. Xu, F.C. Lee, and W.G. Odendaal, "Modeling and Characterization of a 1 KW CCM PFC Converter for Conducted EMI Prediction," *Proceedings of the 19<sup>th</sup> Annual IEEE Applied Power Electronics Conference and Exposition*, pp. 763-769, 2004.
- [6] J.Z. Chen, L. Yang, D. Boroyevich, and W.G. Odendaal, "Essential-coupling-path models for non-contact EMI in switching power converters using lumped circuit elements," *Proceedings of the 19<sup>th</sup> Annual IEEE Applied Power Electronics Conference and Exposition*, pp. 522-525, 2004.
- [7] M.N. Gitau, "Modeling Conducted EMI Noise Generation and Propagation in Boost Converters," *Proceedings of the IEEE International Symposium on Industrial Electronics*, pp. 353-358, 2000.
- [8] N.K. Poon, B.M.H. Pong, C.P. Liu, and C.K. Tse, "Essential-Coupling-Path Models for Non-contact EMI in Switching Power Converters using Lumped Circuit Elements," *IEEE Transactions on Power Electronics*, vol. 18, No. 2, pp. 686-695, 2003.
- [9] T.C.Y. Wang, R. Zhang, J. Sabate, and M. Schutten, "Comprehensive Analysis of Common Mode EMI for Three-Phase UPS System," *Proceedings of the 4<sup>th</sup> International Power Electronics and Motion Control Conference*, vol. 3, pp. 1495-1499, 2004.
- [10] T. Grossen, E. Menzel, and J.H.R. Enslin, "Three-Phase Buck Active Rectifier with Power Factor Correction and Low EMI," *IEE Proceedings on Electric Power Applications*, vol. 146, no. 6, pp. 591-596, 1999.
- [11] IEC International Special Committee on Radio Interference – C.I.S.P.R., "Specification for Radio Interference Measuring Apparatus and Measurement Methods", Publication 16. Genève, Switzerland, 1977.
- [12] International Electrotechnical Commission, "Safety of Information Technology Equipment – IEC 60950," Brussels, Belgium, 1999.